Available online at www.sciencedirect.com
ScienceDirect
Journal of Sound and Vibration 315 (2008) 626–640
JOURNAL OF SOUND AND VIBRATION
www.elsevier.com/locate/jsvi

Non-linear vibrations of laminated cylindrical shallow shells under thermomechanical loading

P. Ribeiro[a,*], E. Jansen[b]

[a]IDMEC/DEMEGI, Faculdade de Engenharia, Universidade do Porto, rua Dr. Roberto Frias, s/n, 4200-465 Porto, Portugal
[b]Faculty of Aerospace Engineering, Delft University of Technology, Kluyverweg 1, 2629 HS Delft, The Netherlands

Accepted 7 January 2008
The peer review of this article was organised by the Guest Editor
Available online 20 February 2008

Abstract

The geometrically non-linear vibrations of linear elastic composite laminated shallow shells under the simultaneous action of thermal fields and mechanical excitations are analysed. For this purpose, a model based on a very efficient *p*-version first-order shear deformation finite element, with hierarchical basis functions, is employed. The equations of motion are solved in the time domain by a Newmark implicit time integration method. The model and code developed are partially validated by comparison with published data. Parametric studies are carried out in order to study the influence of temperature change, initial curvature, panel thickness and fibre orientation on the shells' dynamics.

1. Introduction

Composite laminated shells possess interesting properties like a high stiffness to weight ratio and the possibility to tailor the panel characteristics by selecting the fibre orientation and the stacking sequence of the layers. Therefore, composite laminates are widely used in demanding applications, as for example in aerospace structures, where large dynamic loads occur and the temperature varies [1,2]. In these applications, non-linear, large amplitude, oscillations take place.

A few papers have been published in the area of vibrations of plates and shells under thermomechanical loads and some are referred to here. Reviews on various aspects on the vibration of shells can be found in Refs. [3,4]. Sai Ram and Sinha [5] investigated the effects of moisture and temperature on the linear free vibrations of laminated composite plates using a quadratic isoparametric element, which takes transverse shear into account. It was found that the linear natural frequencies decrease as the moisture and temperature increase. A triangular flat shell finite element was used in Ref. [6] to simulate the geometrically non-linear oscillations of laminated composite plates and shells under the action of heat loads; non-periodic motions were found, with large growth in the vibration amplitude. Mei and co-workers used the finite-element method (FEM) in studies devoted to geometrically non-linear vibrations of panels with thermal fields by combining

*Corresponding author. Tel.: +351 22 508 17 16; fax: +351 22 508 14 45.
E-mail addresses: pmleal@fe.up.pt (P. Ribeiro), E.L.Jansen@tudelft.nl (E. Jansen).

0022-460X/$ - see front matter © 2008 Elsevier Ltd. All rights reserved.
doi:10.1016/j.jsv.2008.01.017

the FEM with modal transformation, in order to reduce the number of degrees of freedom (Refs. [7–9], for example). In Ref. [10], linear vibrations of shear deformable laminated plates exposed to thermomechanical loads and resting on Pasternak-type foundations were analysed. The temperature rise had a small effect on the dynamic response of the plates studied. Ref. [11] deals with hygrothermal effects on the non-linear vibrations of shear deformable, laminated composite plates. A model only with mode (1,1) was employed in the parametric studies. In Ref. [12] a parallel study was carried out, but this focused on the non-linear vibrations of cross-ply laminated plates with piezoelectric actuators and thermal fields. Both in Refs. [11,12], it was concluded that deflections and bending moments increase with temperature, and that, on the other hand, the first linear natural frequency decreases.

Although finite elements have been used to investigate thermomechanical, geometrically non-linear vibrations of laminated panels, to the best of the authors' knowledge, there is no work where this problem was investigated by the *p*-version, hierarchical FEM. This version of the FEM has several advantages over the more widely accepted *h*-version. The reader is referred to Refs. [13–18] and references therein for further details, but it is recalled here that the most important advantage of the *p*-version FEM in non-linear problems is that it generally requires less degrees of freedom.

In this paper, we propose that an efficient *p*-version finite element with hierarchical basis functions, first presented in Ref. [17], is employed to analyse the transient, geometrically non-linear vibration of laminated shallow shells subjected to thermal fields and to mechanical excitations. The equations of motion are solved by Newmark's method. The model and computational codes developed are partially validated by comparing the results with published ones and parametric studies are carried out in order to illustrate the variation of the dynamic response with the temperature, fibre orientation and initial curvature radius.

2. Formulation

If the shell raise is small in comparison with the span, then a relatively simple shallow shell theory can be applied. The derivation of the shallow shell strain displacement relations in linear vibrations can be found in Ref. [19]; here only the essential equations for geometrically non-linear vibrations of shallow shells are presented.

One of the major advantages of the shallow shell theory followed here is that it allows one to employ Cartesian coordinates. The undeformed geometry of the shell is defined from a reference plate by introducing an initial displacement w^1. In terms of a three-dimensional, rectangular coordinate system, which is orientated so that R is the principal curvature, Fig. 1, the middle surface of an open cylindrical shallow shell is expressed as

$$w^1(x,y) = -\frac{1}{2}\left(\frac{y^2}{R}\right). \tag{1}$$

First-order shear deformation theory (FSDT) will be followed for three main reasons: (1) whilst remaining relatively simple, it allows one to investigate moderately thick shells; (2) it allows for a better description of stresses than classical, thin shell theory; and (3) the connection between finite elements is straightforward, as only C_0 continuity is required [20]. Therefore, the displacement components along the in-plane x and y directions—displacements $u(x, y, z, t)$, $v(x, y, z, t)$—at any point of the shell are assumed to be functions of the middle surface

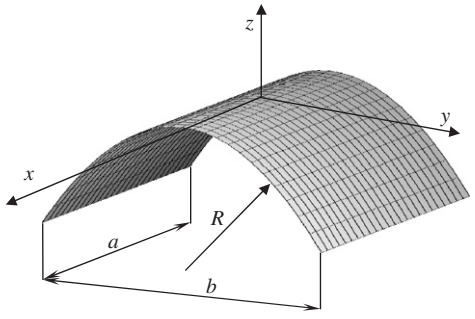

Fig. 1. Representation of an open cylindrical shell.

membrane translations $u^0(x, y, t)$, $v^0(x, y, t)$, and of the independent rotations about the x and y axes, which are, respectively, denoted by $\theta_x^0(x, y, t)$ and $\theta_y^0(x, y, t)$. The displacements are given by:

$$u(x, y, z, t) = u^0(x, y, t) + z\theta_y^0(x, y, t), \tag{2}$$

$$v(x, y, z, t) = v^0(x, y, t) - z\theta_x^0(x, y, t), \tag{3}$$

$$w(x, y, z, t) = w^0(x, y, t), \tag{4}$$

where $w(x, y, z, t)$ and $w^0(x, y, t)$ represent the displacement in the transverse direction, measured in relation to the reference surface.

In each element, the middle plane displacements depend on the local coordinates ξ and η, expressed through the shape functions matrix $\mathbf{N}(\xi,\eta)$, and on the time-dependent vector of generalized displacements $\mathbf{q}(t)$:

$$\begin{Bmatrix} u^0(\xi,\eta,t) \\ v^0(\xi,\eta,t) \\ w^0(\xi,\eta,t) \\ \theta_x^0(\xi,\eta,t) \\ \theta_y^0(\xi,\eta,t) \end{Bmatrix} = \mathbf{N}(\xi,\eta) \begin{Bmatrix} q_u(t) \\ q_v(t) \\ q_w(t) \\ q_{\theta_x}(t) \\ q_{\theta_y}(t) \end{Bmatrix}. \tag{5}$$

When it is necessary to improve the accuracy of the approximation, the number and the order of the shape functions are increased, without re-defining the finite-element mesh. The shape functions used here are the ones employed in Refs. [16–18], which can be consulted for more details; the total numbers of membrane, transverse and rotation shape functions are, respectively, $2p_i{}^2$, $p_0{}^2$ and $2p_\theta{}^2$. Henceforth, the representation of functions will be simplified: for example $u^0(\xi, \eta, t)$ will be represented simply as u^0.

Neglecting the transverse normal stress, the stress–strain relations of an orthotropic lamina, including thermal effects [21], are:

$$\begin{Bmatrix} \sigma_x \\ \sigma_y \\ \sigma_{xy} \end{Bmatrix}^{(k)} = \begin{bmatrix} \overline{Q}_{11} & \overline{Q}_{12} & \overline{Q}_{13} \\ \overline{Q}_{21} & \overline{Q}_{22} & \overline{Q}_{23} \\ \overline{Q}_{31} & \overline{Q}_{32} & \overline{Q}_{33} \end{bmatrix} \left(\begin{Bmatrix} \varepsilon_x \\ \varepsilon_y \\ \gamma_{xy} \end{Bmatrix} - \begin{Bmatrix} \alpha_x \\ \alpha_y \\ 2\alpha_{xy} \end{Bmatrix}^{(k)} \Delta T(z) \right), \tag{6}$$

$$\begin{Bmatrix} \sigma_{yz} \\ \sigma_{xz} \end{Bmatrix}^{(k)} = \begin{bmatrix} \overline{Q}_{44} & \overline{Q}_{45} \\ \overline{Q}_{45} & \overline{Q}_{55} \end{bmatrix} \begin{Bmatrix} \gamma_{yz} \\ \gamma_{xz} \end{Bmatrix},$$

where the transformed coefficients of thermal expansion are given by

$$\begin{Bmatrix} \alpha_x \\ \alpha_y \\ 2\alpha_{xy} \end{Bmatrix}^{(k)} = \begin{bmatrix} \cos^2\theta & \sin^2\theta \\ \sin^2\theta & \cos^2\theta \\ 2\cos\theta\sin\theta & -2\cos\theta\sin\theta \end{bmatrix} \begin{Bmatrix} \alpha_1 \\ \alpha_2 \end{Bmatrix} \tag{7}$$

and the elastic coefficients $\overline{Q}_{ij}$ may be found, for example, in Ref. [19] or Ref. [21]. The symbols α_1 and α_2 in Eq. (7) represent the coefficients of thermal expansion along the principal directions 1 and 2, respectively, while θ represents the angle at which the fibres of the layers are oriented in relation to the x-axis.

The classical shear correction factor $\lambda = 5/6$ is employed here. Ref. [22] provides a comparison between different forms of computing the shear correction factor and it shows that, in most situations, $\lambda = 5/6$ gives rather accurate results. This issue was also addressed in Chapter 2 of Ref. [13], where it was shown that with FSDT and $\lambda = 5/6$ fairly accurate transverse shear stresses of moderately thick ($h/a \leqslant 0.1$) laminated plates are computed. In the present work the relation between the thickness and the projected length (h/a) is not larger than 0.1.

Since constant temperature changes from reference temperatures are of interest here, it will be assumed that the material properties are constant. The parameter ΔT(z) in Eq. (6) represents the temperature change from the temperature of zero thermal stress. A linear variation with z is assumed and therefore the temperature

change is defined as

$$\Delta T(z) = \Delta T_0 + \Delta T_1 \frac{z}{h}, \quad \Delta T_0 = \frac{1}{2}(\Delta T_i + \Delta T_e), \quad \Delta T_1 = \Delta T_e - \Delta T_i, \tag{8}$$

where ΔT_i and ΔT_e represent the change of the temperatures from the temperatures of zero thermal stresses at the surfaces $z = -h/2$ and $h/2$, respectively.

The direct and membrane shear strain components are given by

$$\begin{Bmatrix} \varepsilon_x \\ \varepsilon_y \\ \gamma_{xy} \end{Bmatrix} = \begin{bmatrix} 1 & 0 & 0 & -z & 0 & 0 \\ 0 & 1 & 0 & 0 & -z & 0 \\ 0 & 0 & 1 & 0 & 0 & -z \end{bmatrix} \left(\begin{Bmatrix} \boldsymbol{\varepsilon}^{\mathbf{m}} + \boldsymbol{\varepsilon}^{\mathbf{i}} + \boldsymbol{\varepsilon}^{\mathbf{nl}} \\ \boldsymbol{\varepsilon}^{\mathbf{b}} \end{Bmatrix} \right), \tag{9}$$

where the linear membrane strains, $\boldsymbol{\varepsilon}^{\mathbf{m}}$ and $\boldsymbol{\varepsilon}^{\mathbf{i}}$, the bending strain, $\boldsymbol{\varepsilon}^{\mathbf{b}}$, and the geometrically non-linear membrane strain, $\boldsymbol{\varepsilon}^{\mathbf{nl}}$, are

$$\boldsymbol{\varepsilon}^{\mathbf{m}} = \begin{Bmatrix} u^0_{,x} \\ v^0_{,y} \\ u^0_{,y} + v^0_{,x} \end{Bmatrix}, \quad \boldsymbol{\varepsilon}^{\mathbf{i}} = \begin{Bmatrix} \dfrac{w^0}{R_x} \\ \dfrac{w^0}{R_y} \\ 0 \end{Bmatrix}, \quad \boldsymbol{\varepsilon}^{\mathbf{b}} = \begin{Bmatrix} \dfrac{\partial \theta^0_y}{\partial x} \\ \dfrac{\partial \theta^0_x}{\partial y} \\ \dfrac{\partial \theta^0_y}{\partial y} + \dfrac{\partial \theta^0_x}{\partial x} \end{Bmatrix}, \quad \boldsymbol{\varepsilon}^{\mathbf{nl}} = \begin{Bmatrix} (w^0_{,x})^2/2 \\ (w^0_{,y})^2/2 \\ w^0_{,x} w^0_{,y} \end{Bmatrix}. \tag{10}$$

R_x and R_y represent the principal radius of curvature; since only open cylindrical shells are considered here, either R_x or R_y is infinite. Derivation with respect to x is represented by $(\cdot)_{,x}$ or by $\partial(\cdot)/\partial x$.

The relations between the transverse shear strains, the displacements and the rotations are as follows:

$$\begin{Bmatrix} \gamma_{zx} \\ \gamma_{yz} \end{Bmatrix} = \begin{Bmatrix} w^0_{,x} + \theta_y \\ w^0_{,y} - \theta_x \end{Bmatrix}. \tag{11}$$

Defining the virtual work of the inertia, internal and external forces and applying the principle of the virtual work, the equations of motion are obtained. These equations are:

$$\begin{bmatrix} \mathbf{M}^{11}_u & 0 & 0 & 0 & 0 \\ 0 & \mathbf{M}^{22}_v & 0 & 0 & 0 \\ 0 & 0 & \mathbf{M}^{33}_w & 0 & 0 \\ 0 & 0 & 0 & \mathbf{M}^{44}_{Rx} & 0 \\ 0 & 0 & 0 & 0 & \mathbf{M}^{55}_{Ry} \end{bmatrix} \begin{Bmatrix} \ddot{\mathbf{q}}_u \\ \ddot{\mathbf{q}}_v \\ \ddot{\mathbf{q}}_w \\ \ddot{\mathbf{q}}_{\theta_x} \\ \ddot{\mathbf{q}}_{\theta_y} \end{Bmatrix}$$

$$+ \begin{bmatrix} \mathbf{KL}^{11}_u & 0 & \mathbf{KL}^{13}_{us} & 0 & 0 \\ 0 & \mathbf{KL}^{22}_v & \mathbf{KL}^{23}_{vs} & 0 & 0 \\ \mathbf{KL}^{31}_{su} & \mathbf{KL}^{32}_{sv} & [\mathbf{KL}^{33}_{ss} + \mathbf{KL}^{33}_{\gamma} - \mathbf{K}^{33}_{\Delta T_0} - \mathbf{K}^{33}_{\Delta T_1}] & \mathbf{KL}^{34}_{\gamma} & \mathbf{KL}^{35}_{\gamma} \\ 0 & 0 & \mathbf{KL}^{43}_{\gamma} & \mathbf{KL}^{44}_b + \mathbf{KL}^{44}_{\gamma} & \mathbf{KL}^{45}_b + \mathbf{KL}^{45}_{\gamma} \\ 0 & 0 & \mathbf{KL}^{53}_{\gamma} & \mathbf{KL}^{54}_b + \mathbf{KL}^{54}_{\gamma} & \mathbf{KL}^{55}_b + \mathbf{KL}^{55}_{\gamma} \end{bmatrix} \begin{Bmatrix} \mathbf{q}_u \\ \mathbf{q}_v \\ \mathbf{q}_w \\ \mathbf{q}_{\theta_x} \\ \mathbf{q}_{\theta_y} \end{Bmatrix}$$

$$+\begin{bmatrix} 0 & 0 & \mathbf{KNL}(\mathbf{q}_w)_2^{13} & 0 & 0 \\ 0 & 0 & \mathbf{KNL}(\mathbf{q}_w)_2^{23} & 0 & 0 \\ 2\mathbf{KNL}(\mathbf{q}_w)_2^{13^{\mathrm{T}}} & 2\mathbf{KNL}(\mathbf{q}_w)_2^{23^{\mathrm{T}}} & \mathbf{KNL}(\mathbf{q}_w)_2^{33}+\mathbf{KNL}(\mathbf{q}_w)_{2s}^{33}+2\mathbf{KNL}(\mathbf{q}_w)_2^{33^{\mathrm{T}}} & 0 & 0 \\ 0 & 0 & 0 & 0 & 0 \\ 0 & 0 & 0 & 0 & 0 \end{bmatrix} \begin{Bmatrix} \mathbf{q}_u \\ \mathbf{q}_v \\ \mathbf{q}_w \\ \mathbf{q}_{\theta_x} \\ \mathbf{q}_{\theta_y} \end{Bmatrix}$$

$$= \begin{Bmatrix} \mathbf{P}_u \\ \mathbf{P}_v \\ \mathbf{P}_w \\ \mathbf{M}_{\theta_x} \\ \mathbf{M}_{\theta_y} \end{Bmatrix} + \begin{Bmatrix} \mathbf{F}_u^{\Delta T_0} \\ \mathbf{F}_v^{\Delta T_0} \\ \mathbf{F}_w^{\Delta T_0} \\ \mathbf{M}_{\theta_x}^{\Delta T_0} \\ \mathbf{M}_{\theta_y}^{\Delta T_0} \end{Bmatrix} + \begin{Bmatrix} \mathbf{F}_u^{\Delta T_1} \\ \mathbf{F}_v^{\Delta T_1} \\ \mathbf{F}_w^{\Delta T_1} \\ \mathbf{M}_{\theta_x}^{\Delta T_1} \\ \mathbf{M}_{\theta_y}^{\Delta T_1} \end{Bmatrix}. \tag{12}$$

The constant matrices $\mathbf{M}_k^{ij}$ (where $i = 1$–5 and where k represents any of the matrice's sub-indices) are mass matrices; matrices $\mathbf{KL}_k^{ij}$ are constant stiffness matrices and so are $\mathbf{K}_{\Delta T0}^{33}$ and $\mathbf{K}_{\Delta T1}^{33}$, which are due to the thermal effects. Matrices of type $\mathbf{KNL}(\mathbf{q}_w)_k^{i3}$, where i can be 1, 2 or 3, and $k = 2$ or $k = 2\,\mathrm{s}$, depend linearly on the transverse generalized coordinates $\mathbf{q}_w$ and matrix $\mathbf{KNL}(\mathbf{q}_w)_4^{33}$ depends quadratically on these coordinates. The components of the vector of generalized external forces are: $\mathbf{P}_u$ is the vector of membrane forces in the x direction, $\mathbf{P}_v$ is the vector of membrane forces in the y direction, $\mathbf{P}_w$ is the vector of membrane forces in the z direction, $\mathbf{M}_{\theta_x}$ is the vector of moments about the x-axis and $\mathbf{M}_{\theta_y}$ is the vector of moments about the y-axis.

The matrices and vectors present in the former equation are the ones employed in Ref. [17], with the exception of the matrices and vectors due to the thermal effects. The generalized forces due to ΔT_0 are defined as follows:

$$\mathbf{F}_u^{\Delta T_0} = \Delta T_0 \int_\Omega (A\alpha_x \mathbf{N}_{,x}^u + A\alpha_{xy}\, \mathbf{N}_{,y}^u)\, \mathrm{d}\Omega, \tag{13}$$

$$\mathbf{F}_v^{\Delta T_0} = \Delta T_0 \int_\Omega (A\alpha_y \mathbf{N}_{,y}^v + A\alpha_{xy} \mathbf{N}_{,x}^v)\, \mathrm{d}\Omega, \tag{14}$$

$$\mathbf{F}_w^{\Delta T_0} = \Delta T_0 \frac{A\alpha_x R_y + A\alpha_y R_x}{R_x R_y} \int_\Omega \mathbf{N}^w\, \mathrm{d}\Omega, \tag{15}$$

$$\mathbf{M}_{\theta_x}^{\Delta T_0} = -\Delta T_0 \int_\Omega (B\alpha_y \mathbf{N}_{,y}^{\theta_x} + B\alpha_{xy} \mathbf{N}_{,x}^{\theta_y})\, \mathrm{d}\Omega, \tag{16}$$

$$\mathbf{M}_{\theta_y}^{\Delta T_0} = \Delta T_0 \int_\Omega (B\alpha_x \mathbf{N}_{,x}^{\theta_x} + B\alpha_{xy} \mathbf{N}_{,y}^{\theta_y})\, \mathrm{d}\Omega. \tag{17}$$

The membrane forces $\mathbf{F}_u^{\Delta T_0}$, $\mathbf{F}_v^{\Delta T_0}$ are due to ΔT_0 and $\boldsymbol{\varepsilon}^{\mathbf{m}}$; the transverse force $\mathbf{F}_w^{\Delta T_0}$ is due to ΔT_0 and $\boldsymbol{\varepsilon}^{\mathbf{i}}$; the moments are due to ΔT_0 and to $\boldsymbol{\varepsilon}^{\mathbf{b}}$. Symmetric laminates are under analysis here and $B\alpha_i$ is zero; therefore, moments $\mathbf{M}_{\theta_x}^{\Delta T_0}$ and $\mathbf{M}_{\theta_y}^{\Delta T_0}$ are also zero. Similarly, the force vectors $\mathbf{F}_u^{\Delta T_1}$, $\mathbf{F}_v^{\Delta T_1}$ and $\mathbf{F}_w^{\Delta T_1}$ due to ΔT_1 are zero in symmetric laminates. The moments due to ΔT_1 and $\boldsymbol{\varepsilon}^{\mathbf{b}}$ are given by

$$\mathbf{M}_{\theta_x}^{\Delta T_1} = \frac{\Delta T_1}{h} \int_\Omega (-D\alpha_y \mathbf{N}_{,y}^{\theta_x} - D\alpha_{xy} \mathbf{N}_{,x}^{\theta_x})\, \mathrm{d}\Omega, \tag{18}$$

$$\mathbf{M}_{\theta_y}^{\Delta T_1} = \frac{\Delta T_1}{h} \int_\Omega (D\alpha_x \mathbf{N}_{,x}^{\theta_y} + D\alpha_{xy} \mathbf{N}_{,y}^{\theta_x})\, \mathrm{d}\Omega. \tag{19}$$

In Eqs. (13)–(19) $\mathbf{N}^u$, $\mathbf{N}^v$ and $\mathbf{N}^u$ are the vectors of shape functions associated with the displacement components in the x, y and z directions, respectively. The vectors $\mathbf{N}^{\theta_x}$ and $\mathbf{N}^{\theta_y}$ correspond to the rotations. The terms $A\alpha_i$ and $D\alpha_I$—where $i = x, y, xy$—are defined in the appendix for the sake of completeness.

Matrix $\mathbf{K}^{33}_{\Delta T_1}$ is zero in symmetrical laminates and matrix $\mathbf{K}^{33}_{\Delta T_0}$, which exists because of the geometrical non-linear strain $\boldsymbol{\varepsilon}^{\mathbf{nl}}$ and of ΔT_0, is given by

$$\mathbf{K}^{33}_{\Delta T_0} = \Delta T_0 \int_\Omega (A\alpha_x \mathbf{N}^w_{,x} \mathbf{N}^{w\mathrm{T}}_{,x} + A\alpha_x \mathbf{N}^w_{,y} \mathbf{N}^{w\mathrm{T}}_{,y} + 2A\alpha_{xy} \mathbf{N}^w_{,x} \mathbf{N}^{w\mathrm{T}}_{,y})\, \mathrm{d}\Omega. \tag{20}$$

The mechanical excitations considered here are uniformly distributed and in the z direction. The non-linear equations of motion are solved in the time domain by Newmark's method, with Newmark's parameters [23,24]. This is an implicit method, which allows one to update the non-linear stiffness matrix until the equation

$$\begin{aligned}(\mathbf{K}_\ell + \mathbf{K}_{n\ell}(\mathbf{q}_{t_i+\Delta t}) + a_0\mathbf{M} + a_1\mathbf{C})\mathbf{q}_{t_i+\Delta t} \\ = \mathbf{P}_{t_i+\Delta t} + \mathbf{M}(a_0\mathbf{q}_{t_i} + a_2\dot{\mathbf{q}}_{t_i} + a_3\ddot{\mathbf{q}}_{t_i}) \\ + \mathbf{C}(a_1\mathbf{q}_{t_i} + a_4\dot{\mathbf{q}}_{t_i} + a_5\ddot{\mathbf{q}}_{t_i})\end{aligned} \tag{21}$$

is satisfied below a desired error condition. In the former equation $\mathbf{K}_\ell$ and $\mathbf{K}_{nl}$ stand for the linear and non-linear stiffness matrices, respectively; $\mathbf{M}$ and $\mathbf{C}$ represent the mass and damping matrices. In this work, damping effects are added to the system of equations of motion (12) by introducing a matrix proportional to the linear stiffness matrix, with a factor of proportionality α, i.e. $\mathbf{C} = \alpha\mathbf{K}_\ell$ [23,24]. The vector $\mathbf{P}$ is the vector of external forces. The constants a_0–a_5 are [24]:

$$a_0 = \frac{1}{\gamma\Delta t^2}, \quad a_1 = \frac{\delta}{\gamma\Delta t}, \quad a_2 = \frac{1}{\gamma\Delta t}, \quad a_3 = \frac{1}{2\gamma} - 1, \quad a_4 = \frac{\delta}{\gamma} - 1,$$
$$a_5 = \left(\frac{\delta}{\gamma} - 2\right)\frac{\Delta t}{2}, \quad \delta = 0.5, \quad \gamma = 0.25.$$

The repeated update of the non-linear stiffness matrix until convergence is achieved benefits from the fact that the number of degrees of freedom of the p-version model is rather moderate. Additionally, the number of elements is also smaller than in the h-version of the FEM, reducing the time spent in the assembly stage; actually, for simple geometries as is the case here, just one element is required. The fact that the number of degrees of freedom is not large also means that less time is needed to solve the system of equations that arises in each step of the implicit iterative procedure.

3. Numerical results and comments

3.1. Comparison with published data

In order to partially validate the model used and the computational code implemented a few comparisons with published results were carried out. First, linear vibrations were considered and the frequency parameters $\Omega = \omega a^2\sqrt{\rho/E_1h^2}$ of a completely free, moderately thin ($a/h = 100$) shallow shell of square planform ($a/b = 1$) analysed in Refs. [19,25] were computed. In the code, geometric boundary conditions are imposed and in the case of free boundaries all middle surface displacements and rotations are unrestrained, which should correspond to zero membrane forces and moments at the boundaries. The stacking sequence is $[30^\circ/-30^\circ/-30^\circ/30^\circ]$, where the angle lies between the fibres and the projection of the x-axis upon the shell. The relation between the projected span and the radius is $a/R = 0.5$ and the material properties are the ones of Refs. [19,25] for graphite-epoxy: $E_1 = 138.0\,\mathrm{GPa}$, $E_2 = 8.96\,\mathrm{GPa}$, $G_{12} = 7.1\,\mathrm{GPa}$ and $v_{12} = 0.30$. Because thin plate theory was followed in those references, G_{13} and G_{23} were not given and will be made equal to G_{12} here, as is done in other examples presented in Ref. [19]. Moreover, the mass density was assumed to be $\rho = 1600\,\mathrm{kg\,m^{-3}}$.

Table 1 shows that with the p-version finite element $p_o = p_i = p_\theta = 7$ the natural frequencies are very close to the ones given in Refs. [19,25] and that with the element $p_o = p_i = p_\theta = 8$ lower values are obtained for all

Table 1
Frequency parameter of a graphite epoxy [30°/−30°/−30°/30] completely free shallow shell; $a/R = 0.5$, $a/b = 1$, $a/h = 100$

	dof	Mode number							
		1	2	3	4	5	6	7	8
p-Version, $p_o = 7$, $p_i = 7$, $p_\theta = 7$	245	2.2137	5.1271	5.5641	7.6941	7.9948	12.847	13.263	14.243
p-Version, $p_o = 8$, $p_i = 8$, $p_\theta = 8$	320	2.2110	5.1171	5.5561	7.6590	7.9690	12.506	12.930	13.963
p-Version, $p_o = 10$, $p_i = 10$, $p_\theta = 8$	428	2.2109	5.1162	5.5544	7.6551	7.9614	12.489	12.900	13.938
p-Version, $p_o = 8$, $p_i = 10$, $p_\theta = 10$	464	2.2092	5.1161	5.5513	7.6497	7.9601	12.483	12.902	13.942
p-Version, $p_o = 10$, $p_i = 8$, $p_\theta = 10$	428	2.2091	5.1158	5.5509	7.6495	7.9585	12.494	12.903	13.939
p-Version, $p_o = 10$, $p_i = 10$, $p_\theta = 10$	500	2.2091	5.1156	5.5505	7.6470	7.9570	12.479	12.885	13.924
Refs. [19,25], thin shell theory	192	2.2156	5.1241	5.5678	7.6824	7.9914	12.551	12.982	13.997

Table 2
Frequency parameter $\Omega = \omega a^2\sqrt{\rho/E_2h^2}$ of a [0°/90°/90°/0°] simply supported plate, $a/b = 1$, $a/h = 100$, $\Delta T_0 = 25\,\mathrm{K}$, $\Delta T_1 = 0$

Deflection mode	Sai Ram and Sinha [5]	Huan et al. [11]	Parhi et al. [26]	p-Version FEM
(1,1)	8.088	8.043	8.046	8.0453
(1,2)	19.196	18.140	18.350	18.332
(2,1)	39.324	38.364	38.590	38.550

natural frequencies computed. It is natural that the present approach yields lower values, since FSDT provides lower frequencies than thin shell theory. On the other hand, because in FSDT the rotations require additional variables, the FSDT p-element approach requires more degrees of freedom—yet still a moderate number—than the model employed in Refs. [19,25].

Table 1 also shows that the importance of the different shape functions and coordinates—that is, of p_i, p_o and p_θ—depends on the mode in question. For example, with $p_o = 10$, $p_i = 8$, $p_\theta = 10$ the first five natural frequencies are lower than with $p_o = 10$, $p_i = 10$, $p_\theta = 8$ and $p_o = 8$, $p_i = 10$, $p_\theta = 10$, but the sixth and seventh natural frequencies are higher (the linear natural frequency converges from above in the p-version FEM if a hierarchic set of functions is used). In most of the following numerical examples p_o, p_i and p_θ are equal.

Since it is apparently easier to find published results on plates than on shells for the problem at hand, the ensuing comparisons are on plates. The next comparison concerns the linear natural frequencies of a graphite/epoxy, square laminated thin plate ($b/h = 100$), simply supported with no membrane displacements at all boundaries (for example at $\xi = -1$ the imposed boundary conditions are $u^0(-1, \eta, t) = v^0(-1, \eta, t) = w^0(-1, \eta, t) = 0$, $\theta_x^0(-1, \eta, t) = 0$ and the rotation about the y-axis is free). The plate is at a uniform temperature T_0 equal to 325 K, increasing from a uniform temperature for zero thermal stress equal to 300 K ($\Delta T_0 = 25\,\mathrm{K}$, $\Delta T_1 = 0\,\mathrm{K}$). The properties of the lamina are [5]: $E_1 = 130.0\,\mathrm{GPa}$, $E_2 = 9.5\,\mathrm{GPa}$, $G_{12} = G_{13} = 6.0\,\mathrm{GPa}$, $G_{23} = 0.5$, G_{12}, $v_{12} = 0.30$ and $\alpha_{11} = -0.3 \times 10^{-6}\,\mathrm{K}^{-1}$, $\alpha_{22} = 28.1 \times 10^{-6}\,\mathrm{K}^{-1}$. We could not find the value of ρ in Ref. [5] and used $1600\,\mathrm{kg\,m}^{-3}$. The values of the frequency parameters computed in different references are given in Table 2 and the agreement is close.

Next, the response of an undamped and moderately thick plate investigated in Ref. [10] is examined. The four plate edges are simply supported with no membrane displacements. The uniform temperature increase from the temperature for zero thermal stresses is $\Delta T_0 = 200\,\mathrm{K}$ and the properties of each lamina are $E_2 = 6.895\,\mathrm{GPa}$, $E_1/E_2 = 40$, $G_{12}/E_2 = G_{13}/E_2 = 0.6$, $G_{23}/E_2 = 0.5$, G_{12}, $v_{12} = 0.25$ and $\alpha_{11} = -1.14 \times 10^{-6}\,\mathrm{K}^{-1}$, $\alpha_{22} = 11.4 \times 10^{-6}\,\mathrm{K}^{-1}$. The thickness of the plate is 50.8 mm and $a = b = 10\,h$. Probably there is a typographical mistake in the value of the mass density given in Ref. [10], which is not realistic, and here it was assumed that $\rho = 1389.23\,\mathrm{kg\,m}^{-3}$ from another example of the same reference.

In this case, the frequency parameters $\Omega = \omega a^2\sqrt{\rho/E_2h^2}$ computed with the p-version model at $\Delta T_0 = 0$ and $\Delta T_0 = 200\,\mathrm{K}$ are 14.434 and 14.021, respectively. These values are close to the ones given in Ref. [10],

which are 14.702 ($\Delta T_0 = 0$ K) and 14.490 ($\Delta T_0 = 200$ K). A load that is zero at $t = 0^-$ s and is equal to $q(x, y, t) = q_0 \sin(\pi x/a) \sin(\pi y/b)$, with $q_0 = 34.48$ MPa, for $t > 0$ s is applied and the response computed with the p-model is shown in Fig. 2; it is similar to the one given in Fig. 3 of Ref. [10], although there is a small difference in the time taken between minimum displacements. This small difference may be due to the value of ρ which is unclear as explained.

A simply supported square plate with immovable edges, isotropic, undamped and vibrating in the geometrically non-linear regime due to a suddenly applied distributed transverse load is the subject of the following example. The geometric material and load parameters are the ones given in Ref. [27]: $a = b = 2.438$ m, $h = 0.00635$ m, $\rho = 254.7\,\mathrm{kg\,m^{-3}}$ (Ref. [27] gives $\rho = 2.547 \times 10^{-6}\,\mathrm{N\,s^2\,cm^{-4}}$), $E_1 = E_2 = 7.031 \times 10^9\,\mathrm{N\,m^{-2}}$ and $v_{12} = 0.25$. The response to load $q = 24.41\,\mathrm{N\,m^{-2}}$ is given in Fig. 3. The maximum amplitude displacement attained is 1.21×10^{-2} m, which is fairly close to the one presented in Refs. [27,28].

Finally, a three-layered, [45°/−45°/45°], undamped, fully clamped plate (for example, at $\xi = -1$, the imposed boundary conditions are $u^0(-1, \eta, t) = v^0(-1, \eta, t) = w^0(-1, \eta, t) = 0$, $\theta_x^0(-1, \eta, t) = \theta_y^0(-1, \eta, t) = 0$) investigated in Refs. [15,18,29] is analysed. The properties are: $a = b = 0.5$ m, $h = 5 \times 10^{-3}$ m, $\rho = 2564.856\,\mathrm{kg\,m^{-3}}$, $E_1 = 206.84\,\mathrm{GN\,m^{-2}}$, $E_2 = 5.171\,\mathrm{GN\,m^{-2}}$, $G_{12} = 2.5855\,\mathrm{GN\,m^{-2}}$ and $v_{12} = 0.25$, and

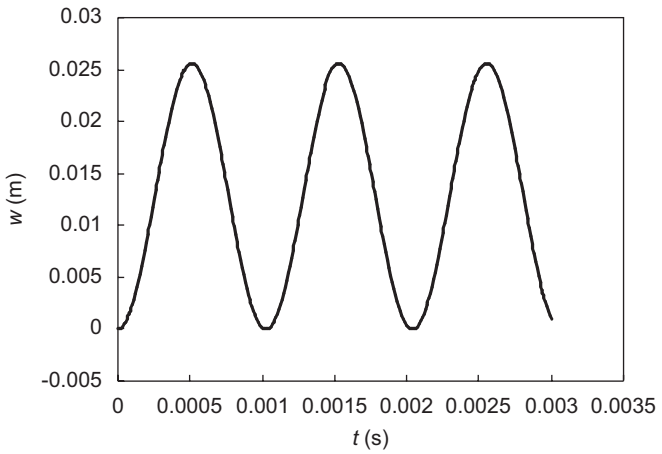

Fig. 2. Transverse displacement of the central point of the [0°/90°/0°] laminated square plate versus time.

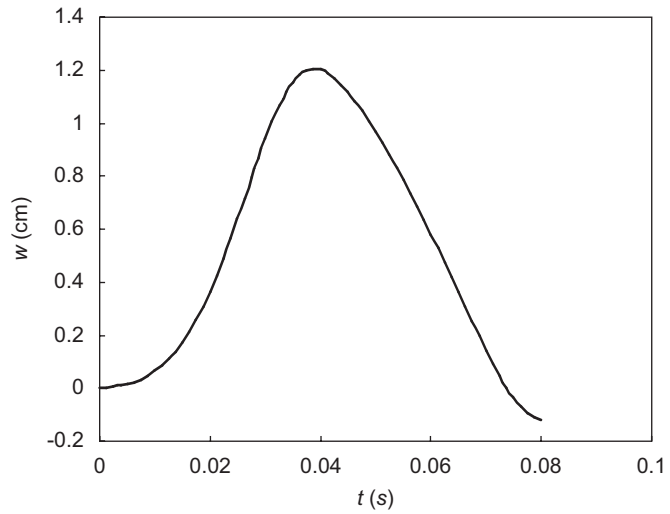

Fig. 3. Transverse displacement of the central point of an isotropic plate under a suddenly applied uniformly distributed load.

the excitation is provided by a distributed force of $3454.665\,\mathrm{N\,m^{-2}}$ amplitude, which varies sinusoidaly with time. In order to dissipate transients a small damping parameter ($\alpha = 10^{-6}$) was introduced into the present model. Table 3 shows that the relations between the amplitude displacement and excitation frequency computed with the present approach agree with the ones of the other references. Resemblance is particularly close to the results of Ref. [18], where a similar model was employed, but where the membrane inertia was neglected and the equations of motion were solved by the shooting method.

3.2. Parametric studies

In the previous section, close agreement between the results of the present approach and the published ones was verified. The method is now applied to carry out parametric studies in non-linear, transient vibrations of cylindrical, symmetrically laminated shallow shells with the goal of providing an insight into how the different parameters affect the dynamic behaviour of the laminated shells.

The boundaries in all the ensuing examples are simply supported and immovable, that is $u^0(-a/2,y,t) = u^0(a/2,y,t) = u^0(x,-b/2,t) = u^0(x,b/2,t) = 0$; similar conditions hold for $v^0(x,y,t)$ and the moments about the boundary axis are zero. The initial conditions are zero displacement and zero velocity. The material properties employed are the ones given in Ref. [9] for a graphite-epoxy lamina: $E_1 = 155\,\mathrm{GPa}$, $E_2 = 8.1\,\mathrm{GPa}$, $G_{12} = 4.6\,\mathrm{GPa}$, $\rho = 1550\,\mathrm{kg\,m^{-3}}$, $v_{12} = 0.22$, $\alpha_1 = -0.07200 \times 10^{-6}\,\mathrm{K^{-1}}$ $(-0.04 \times 10^{-6}\,\mathrm{F^{-1}})$ and $\alpha_2 = 3.00761 \times 10^{-5}\,\mathrm{K^{-1}}$ $(1.67 \times 10^{-5}\,\mathrm{F^{-1}})$. Here it was assumed that $G_{13} = G_{23} = G_{12}$. The reference dimensions of the panel are also from Ref. [9]: thickness $h = 0.0012192\,\mathrm{m}$ (0.048 in) and quadrangular planform $a = b = 0.3048\,\mathrm{m}$ (12 in), that is $a/h = 250$. Thickness and curvature radius will change in some tests. The damping parameter α is defined as $\alpha = 0.01/\omega_{\ell_1}$, where 0.01 is the value employed for a non-dimensional damping coefficient of laminated shells in Ref. [30] and ω_{ℓ_1} is the first linear natural frequency. The excitation amplitudes are selected so that the panels experience non-linear behaviour but, with few exceptions, the displacement amplitudes remain within twice the panel thickness ($2h$). This is the widely accepted limit for Von Kármán's theory to remain valid, although Von Kármán relations have provided good results at larger amplitudes [31]. The $2h$ boundary will only be passed in two cases, in order to show the evolution of the dynamic behaviour with the specific parameter under consideration.

In the first example of this section, and to investigate the influence of the curvature on the response, three relations between the initial curvature radius and the projected length are considered: $b/R = 0$, 0.2 and 0.4. In the three cases the lamination sequence is $[0^\circ/45^\circ/-45^\circ/90^\circ]_s$. The mechanical excitation is provided by a suddenly applied distributed transverse load of finite duration $t_1 = 0.05\,\mathrm{s}$ and amplitude $q_0 = -500\,\mathrm{N\,m^{-2}}$ (Fig. 4). The critical buckling temperature computed for the simply supported plate with the present model is $\Delta T_0 = 10.89\,\mathrm{K}$, which is rather close to the value given in Ref. [9] ($\Delta T_0 = 10.95\,\mathrm{K}$). In the case of shells $b/R = 0.2$ and $b/R = 0.4$, the critical buckling temperature is $\Delta T_0 = 38.93$ and $69.74\,\mathrm{K}$, respectively.

Fig. 5 shows the responses of these three panels at different temperatures. When $\Delta T_0 = -50\,\mathrm{K}$ the plate stiffens due to the induced tensional stresses and therefore experiences lower amplitude vibrations than in the other cases. At $\Delta T_0 = -50$ and $0\,\mathrm{K}$ the plate experiences oscillations around the flat equilibrium configuration, because these temperatures are below the critical buckling temperature. On the other hand, shells $b/R = 0.2$ and 0.4 oscillate around inwardly deformed configurations when $\Delta T_0 = -50\,\mathrm{K}$. This is due to

Table 3
Amplitude of vibration of a $[45^\circ/-45^\circ/45]$ plate at point ($\xi = 0$, $\eta = 0$) as a function of ω/ω_{ℓ_1}

	HFEM, thin plate theory [15]		FEM, thin plate theory [29]	FSDT [18] $p_o = 4$, $p_i = 8$, $p_\theta = 6$	Present, $p_o = 4$, $p_i = 8$, $p_\theta = 6$
$W_{\max}/h$	ω/ω_{ℓ_1}	$W_{\max}/h$	ω/ω_{ℓ_1}	ω/ω_{ℓ_1}	ω/ω_{ℓ_1}
0.20163	0.73401	0.2000	0.7219	0.7268	0.7268
0.59965	1.00845	0.6000	1.0085	1.005	1.005

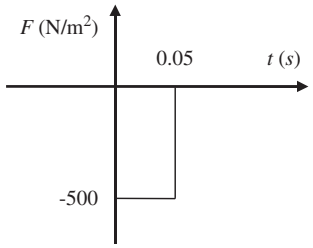

Fig. 4. Amplitude of distributed force.

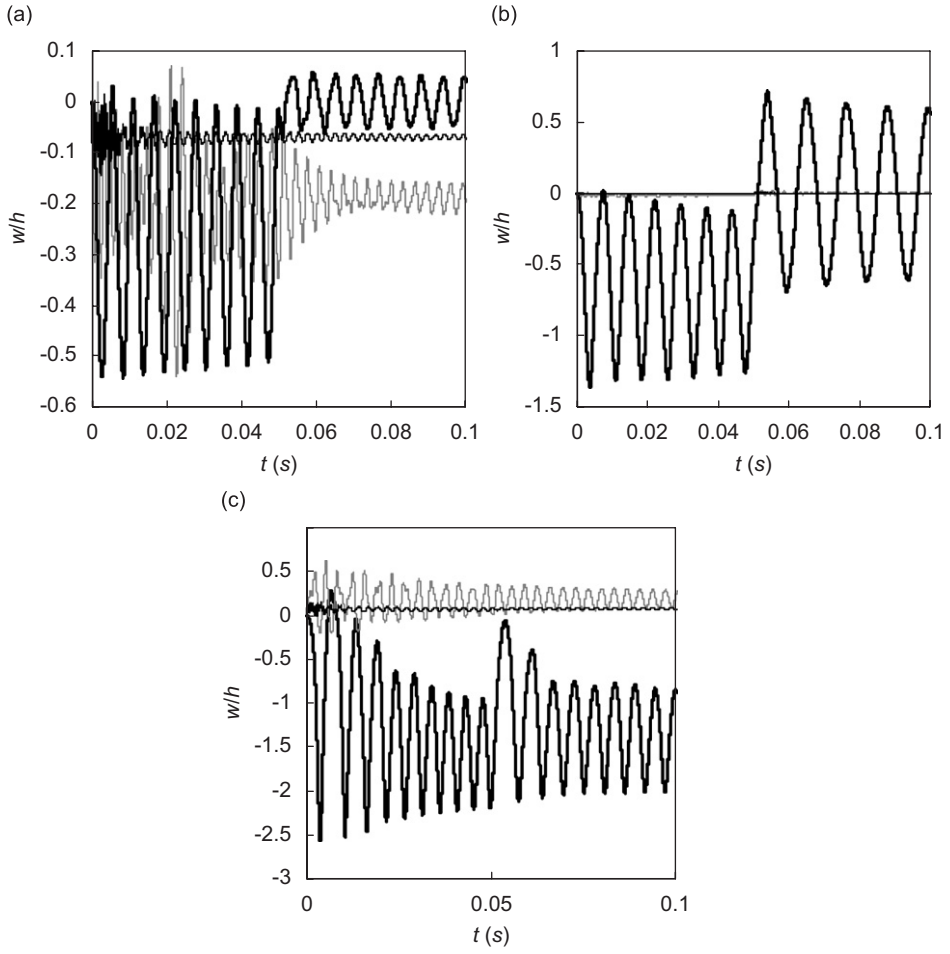

Fig. 5. Transverse displacement of central point of panels under a rectangular impulse, $-500\,\mathrm{N\,m^{-2}}$; ▬ plate, ▬ shell $b/R = 0.2$ and — shell $b/R = 0.4$, (a) $\Delta T_0 = -50\,\mathrm{K}$, (b) $\Delta T_0 = 0\,\mathrm{K}$, (c) $\Delta T_0 = 50\,\mathrm{K}$.

the induced inward force $\mathbf{F}_w^{\Delta T_0}$, which contracts the shell decreasing its curvature. This force only exists on shells as Eq. (15) shows. When $\Delta T_0 = 0\,\mathrm{K}$ both shells experience very small amplitude oscillations. When $\Delta T_0 = 50\,\mathrm{K}$, the plate oscillates around a non-flat equilibrium configuration, because the temperature is above its critical buckling temperature. Unlike the plate, shells $b/R = 0.2$ and 0.4 oscillate around outwardly deformed configurations due to force $\mathbf{F}_w^{\Delta T_0}$, which in this case acts outwards. At the three temperatures considered, shell $b/R = 0.4$ experiences rather low-amplitude vibrations for two connected reasons: its critical buckling temperature is above 50 K and this shell is stiffer due to its larger initial curvature than the other

panels; therefore, it does not deform so much under a similar mechanical force. Being stiffer and with more or less the same mass as the other panels, shell $b/R = 0.4$ has higher natural frequencies, and therefore undergoes higher-frequency oscillations at the three temperatures.

Fig. 6 shows the transverse displacement of the central point of $[0/\theta/-\theta/2\theta]_s$ panels under rectangular impulse, uniformly distributed, with $-500\,\mathrm{N\,m^{-2}}$. Three uniform temperature fields defined by $\Delta T_1 = 0\,\mathrm{K}$ and $\Delta T_0 = -50$, 0 or 50 K are considered and the fibre orientation can be $\theta = 0^\circ$, 30°, 45° or 60°. This example demonstrates the large influence that the lay-up may have on the dynamic behaviour of a laminate, being observable that the shell with all fibres in the same direction ($\theta = 0^\circ$) experiences much larger amplitudes of vibration than any of the other shells. Shell $\theta = 45^\circ$ experiences the lowest vibration amplitudes, because this is the more balanced lay-up in $[0/\theta/-\theta/2\theta]_s$ panels. Whichever the fibre orientation, if there is a temperature change, force $\mathbf{F}_w^{\Delta T_0}$ obliges the shells to oscillate around an equilibrium configuration which differs from the original configuration. This force of thermal origin also exists after instant $t = 0.05\,\mathrm{s}$, when the mechanical force becomes zero, and in actual fact changes the geometry of the shell. Thus, one could consider that the thermal force is causing an imperfection in the geometry, although in this case it is not a stress free imperfection.

To examine the effect of the thickness on the response, another length to thickness ratio is considered here, namely $a/h = 10$. The amplitude of the excitation is defined as $q_0 = -500\,(250\,a/h)^3\,\mathrm{N\,m^{-2}}$, because the terms of the bending stiffness matrix **D** involve the cube of the thickness. Fig. 7 shows that the thin shell is much

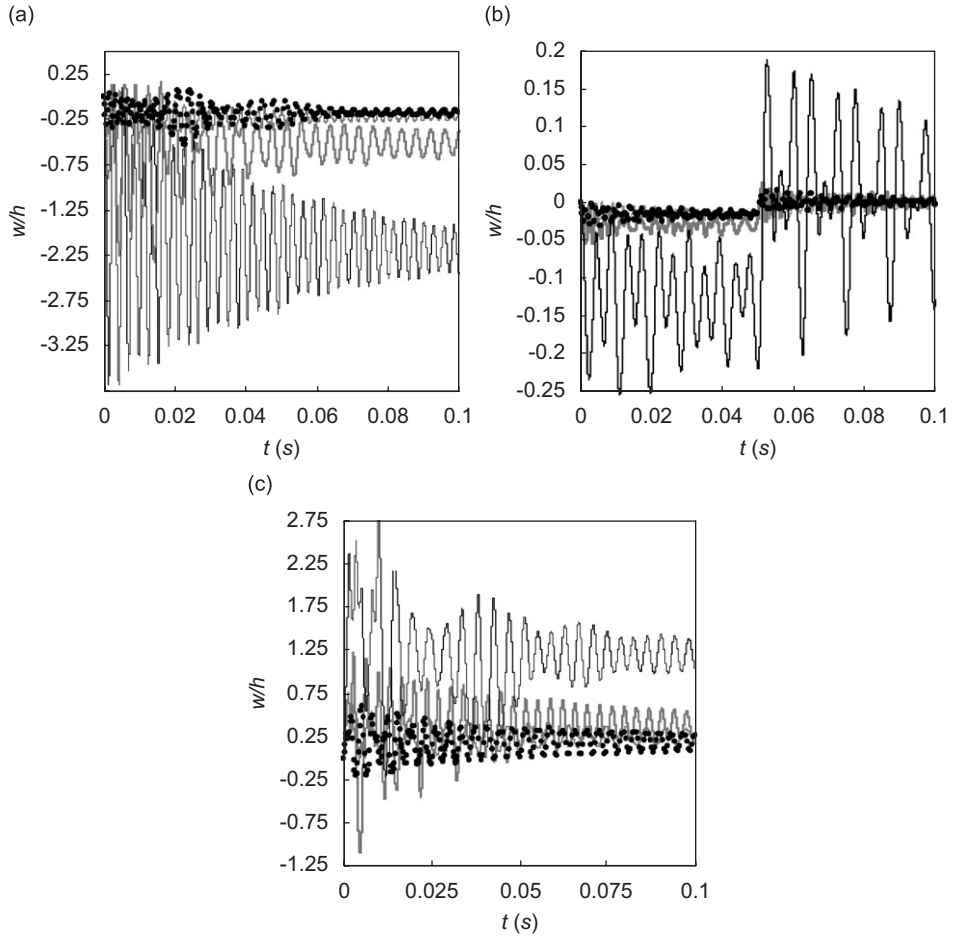

Fig. 6. Transverse displacement of the central point of a $[0/\theta/-\theta/2\theta]$ shell $b/R = 0.2$, under a rectangular impulse distributed uniformly, with $-500\,\mathrm{N\,m^{-2}}$: (a) $\Delta T_0 = -50\,\mathrm{K}$, (b) $\Delta T_0 = 0\,\mathrm{K}$, (c) $\Delta T_0 = 50\,\mathrm{K}$; — $\theta = 0^\circ$, ▬ $\theta = 30^\circ$, ●●● $\theta = 45^\circ$, — $\theta = 60^\circ$.

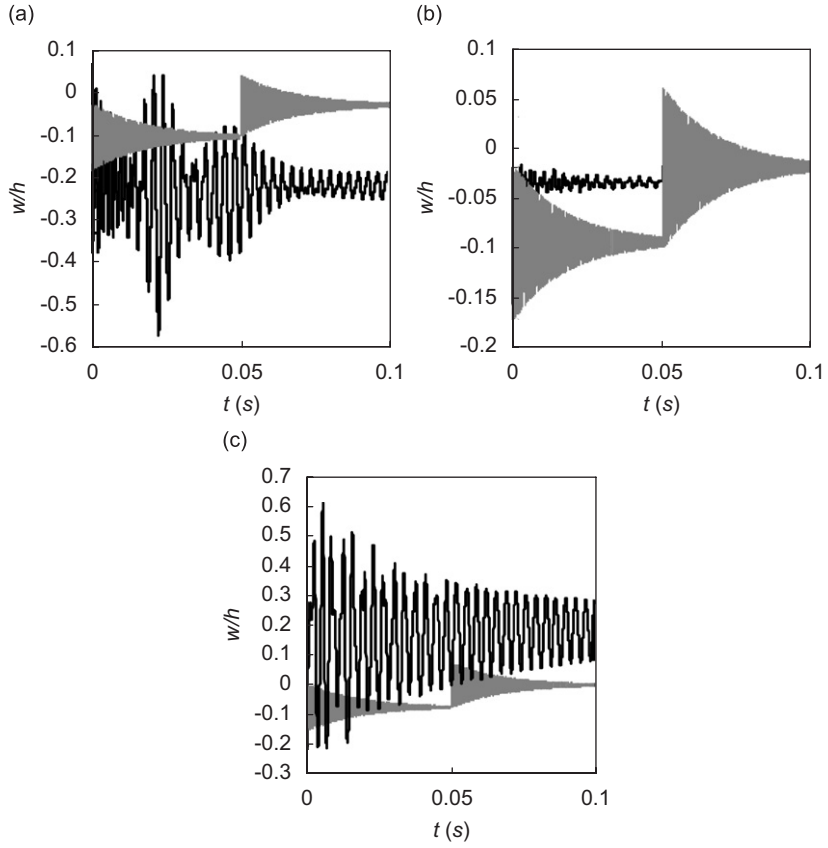

Fig. 7. Transverse displacement of the central point of panels under a rectangular impulse, uniformly distributed, with $-500\,\mathrm{N\,m^{-2}}$; shell $b/R = 0.2$, ▬ thin, ▬ thick, (a) $\Delta T_0 = -50\,\mathrm{K}$, (b) $\Delta T_0 = -0\,\mathrm{K}$, (c) $\Delta T_0 = -50\,\mathrm{K}$.

more affected by the temperature changes than the thick one. In the latter, the dynamic response is only marginally altered by temperature variations and the mechanical load is more important, hence the very visible change in the response when the mechanical load becomes zero. The thick shell experiences oscillations at higher frequencies, because its natural frequencies are higher than the ones of the thin shell.

Finally, we consider the case where $\Delta T_1 \neq 0\,\mathrm{K}$ and therefore where the moments defined by Eqs. (18) and (19) are not zero. Numerical tests are carried out on shell $b/R = 0.4$, $[0^\circ/45^\circ/-45^\circ/90^\circ]_s$, the mechanical excitation is provided by an impulsive distributed force of $-1000\,\mathrm{N\,m^{-2}}$, with duration 0.05 s. Fig. 8 shows the responses when the temperature change in the inner surface of the shell, ΔT_i, is smaller than or equal to than the temperature change in the outer surface of the shell, ΔT_e; the average temperature, ΔT_0, is always 50 K. It results from these tests that the positive temperature variation with the coordinate z, which is linked to a relative contraction of the inner layers with respect to the outer layers, has a stiffening effect. The inverse phenomenon is observed in Fig. 9, where $\Delta T_i > \Delta T_e$.

4. Conclusions

A p-version shell finite element with hierarchic functions and that accounts for shear deformation and rotary inertia was applied to study oscillations of laminated shallow shells under transverse excitations and thermal fields. The model and computational code were validated by comparison with published data.

The set of parametric studies carried out yielded information that may be useful to designers. One of the immediate conclusions of interest is that, clearly, even rather moderate temperature changes strongly facilitate

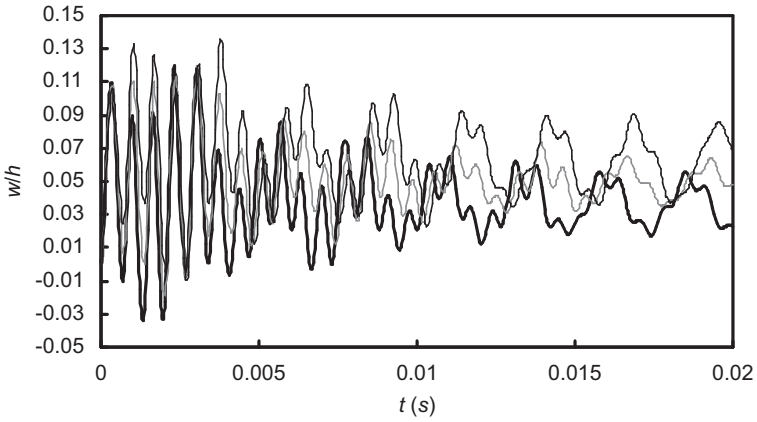

Fig. 8. Transverse displacement of the central point of panels under a rectangular impulse, uniformly distributed, with $-1000\,\mathrm{N\,m^{-2}}$; shell $b/R = 0.4$, ▬ $\Delta T_i = 30$, $\Delta T_e = 70$, — $\Delta T_i = 40$, $\Delta T_e = 60$, — $\Delta T_i = 50$, $\Delta T_e = 50$.

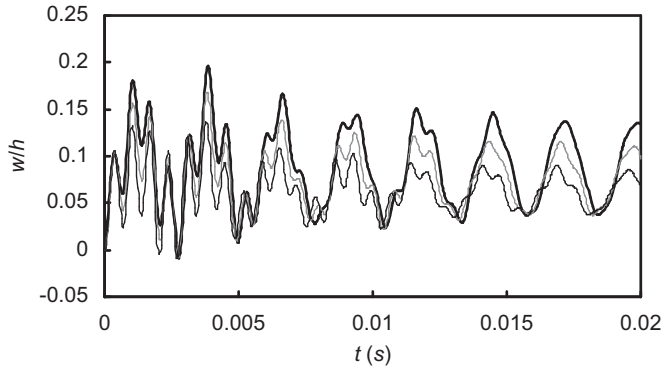

Fig. 9. Transverse displacement of the central point of panels under a rectangular impulse, uniformly distributed, with $-1000\,\mathrm{N\,m^{-2}}$; shell $b/R = 0.4$, ▬ $\Delta T_i = 70$, $\Delta T_e = 30$, — $\Delta T_i = 60$, $\Delta T_e = 40$, — $\Delta T_i = 50$, $\Delta T_e = 50$.

the appearance of large amplitude vibrations. In plates, the equilibrium configuration only changes when thermally induced buckling occurs. In shells the equilibrium configuration is always transformed by temperature changes altering the reference geometry, even if there is no buckling. It was also verified that the fibre orientation has a strong influence on the thermomechanical behaviour of shells, being evident that the limit case of shells where all fibres have the same direction experiences much larger amplitude oscillations than other shells. The panel thickness is another parameter of paramount importance for the dynamics, as thick shells are much less influenced by temperature changes than thinner ones. Finally, it was verified that different temperature gradients through the thickness, with the same average temperature, cause quite different vibration amplitudes.

Acknowledgements

The first author acknowledges the Aerospace Structures Group, Faculty of Aerospace Engineering, Technical University of Delft, where part of this work was carried out, and the sabbatical grant SFRH/BSAB/582/2006 from the Fundação para a Ciência e a Tecnologia, Portugal.

Appendix. Vectors Aα and Dα

The vectors **Aα** and **Dα** are, respectively, given by

$$\begin{Bmatrix} A\alpha_x \\ A\alpha_y \\ A\alpha_{xy} \end{Bmatrix} = \sum_{k=1}^{n} \int_{h_{k-1}}^{h_k} \begin{bmatrix} \overline{Q}_{11} & \overline{Q}_{12} & \overline{Q}_{16} \\ \overline{Q}_{12} & \overline{Q}_{22} & \overline{Q}_{26} \\ \overline{Q}_{16} & \overline{Q}_{26} & \overline{Q}_{66} \end{bmatrix} \begin{bmatrix} \cos^2\theta_k & \sin^2\theta_k \\ \sin^2\theta_k & \cos^2\theta_k \\ 2\sin\theta_k\cos\theta_k & -2\sin\theta_k\cos\theta_k \end{bmatrix} \begin{Bmatrix} \alpha_{11} \\ \alpha_{22} \end{Bmatrix} \mathrm{d}z, \tag{22}$$

$$\begin{Bmatrix} D\alpha_x \\ D\alpha_y \\ D\alpha_{xy} \end{Bmatrix} = \sum_{k=1}^{n} \int_{h_{k-1}}^{h_k} z^2 \begin{bmatrix} \overline{Q}_{11} & \overline{Q}_{12} & \overline{Q}_{16} \\ \overline{Q}_{12} & \overline{Q}_{22} & \overline{Q}_{26} \\ \overline{Q}_{16} & \overline{Q}_{26} & \overline{Q}_{66} \end{bmatrix} \begin{bmatrix} \cos^2\theta_k & \sin^2\theta_k \\ \sin^2\theta_k & \cos^2\theta_k \\ 2\sin\theta_k\cos\theta_k & -2\sin\theta_k\cos\theta_k \end{bmatrix} \begin{Bmatrix} \alpha_{11} \\ \alpha_{22} \end{Bmatrix} \mathrm{d}z, \tag{23}$$

where $\overline{Q}_{ij}$ are the transformed elastic coefficients referred to the (x, y, z) coordinate system, θ_k is the angle between the fibre direction of the k lamina and the x-axis and α_{11} and α_{22} are the coefficients of thermal expansion in the principal directions of each lamina. For further details the reader is invited to consult Ref. [21].

References

[1] E.A. Thorton, *Thermal Structures for Aerospace Applications*, AIAA Education Series, Reston, 1996.

[2] C. E. Harris, M. J. Shuart, H. R. Gray, A Survey of Emerging Materials for Revolutionary Aerospace Vehicle Structures and Propulsion Systems. NASA/TM-2002-211664, 2002.

[3] K.M. Liew, C.W. Lim, S. Kitipornchai, Vibration of shallow shells: a review with bibliography, *Applied Mechanics Reviews* 50 (1997) 431–444.

[4] M. Amabili, M.P. Paidoussis, Review of studies on geometrically Non-linear vibrations and dynamics of circular cylindrical shells and panels, with and without fluid–structure interaction, *Applied Mechanics Reviews* 56 (2003) 349–381.

[5] K.S. Sai Ram, P.K. Sinha, Hygrothermal effects on the free vibration of laminated composite plates, *Journal of Sound and Vibration* 158 (1992) 133–148.

[6] J.H. Argyris, L. Tenek, Non-linear and chaotic oscillations of composite plates and shells under periodic heat load, *Computer Methods in Applied Mechanics and Engineering* 122 (1995) 351–377.

[7] Y.C. Shi, R.Y.Y. Lee, C. Mei, Thermal postbuckling of composite plates using the finite element modal coordinate method, *Journal of Thermal Stresses* 22 (1999) 595–614.

[8] J.M. Dhainaut, X.Y. Guo, C. Mei, S.M. Spottswood, H.F. Wolfe, Non-linear random response of panels in an elevated thermal–acoustic environment, *Journal of Aircraft* 40 (2003) 683–691.

[9] G. Cheng, C. Mei, Finite element modal formulation for hypersonic panel flutter analysis with thermal effects, *AIAA Journal* 42 (2004) 687–695.

[10] H.-S. Shen, J.-J. Zheng, X.-L. Huang, Dynamic response of shear deformable laminated plates under thermomechanical loading and resting on elastic foundations, *Composite Structures* 60 (2003) 57–66.

[11] X.-L. Huang, H.-S. Shen, J.-J. Zheng, Non-linear vibration and dynamic response of shear deformable laminated plates in hygrothermal environments, *Composite Science and Technology* 64 (2004) 1419–1435.

[12] X.-L. Huang, H.-S. Shen, Non-linear free and forced vibrations of simply supported shear deformable laminated plates with piezoelectric actuactors, *International Journal of Mechanical Sciences* 47 (2005) 187–208.

[13] W. Han, The Analysis of Isotropic And Laminated Rectangular Plates including Geometrical Non-linearity using the *p*-Version Finite Element Method, PhD Thesis, University of Southampton, 1993.

[14] W. Han, M. Petyt, Geometrically Non-linear vibration analysis of thin, rectangular plates using the hierarchical finite element method—II: 1st mode of laminated plates and higher modes of isotropic and laminated plates, *Computers and Structures* 63 (1997) 309–318.

[15] P. Ribeiro, M. Petyt, Non-linear vibration of composite laminated plates by the hierarchical finite element method, *Composite Structures* 46 (1999) 197–208.

[16] P. Ribeiro, A hierarchical finite element for geometrically Non-linear vibration of doubly curved, moderately thick isotropic shallow shells, *International Journal for Numerical Methods in Engineering* 56 (2003) 715–738.

[17] P. Ribeiro, Forced Non-linear vibration of cylindrical laminated shells by the *p*-version finite element method, *Proceedings of the 45th AIAA/ASME/ASCE/AHS/ASC Stru ctures, Structural Dynamics & Materials Conference*, California, 2004, AIAA 2004-1865.

[18] P. Ribeiro, Forced periodic vibrations of laminated composite plates by a *p*-version, first order shear deformation, finite element, *Composite Science and Technology* 66 (2006) 1844–1856.

[19] M.S. Qatu, *Vibration of Laminated Shells and Plates*, Elsevier, Amsterdam, 2004.

[20] O.C. Zienkiewicz, R.L. Taylor, *The Finite Element Method*, fifth ed., Butterworth-Heinemann, Oxford, 2000.

[21] J.N. Reddy, *Mechanics of Laminated Composite Plates and Shells: Theory and Analysis*, CRC Press, Boca Raton, FL, 2004.
[22] A.K. Noor, W.S. Burton, Predictor–corrector procedure for stress and free vibration analyses of multilayered composite plates and shells, *Computer Methods in Applied Mechanics and Engineering* 82 (1990) 341–363.
[23] M. Petyt, *Introduction to Finite Element Vibration Analysis*, Cambridge University Press, Cambridge, 1990.
[24] K.-J. Bathe, *Finite Element Procedures*, Prentice-Hall, Upper Saddle River, 1996.
[25] M.S. Qatu, A.W. Leissa, Free vibrations of completely free doubly curved laminated composite shallow shells, *Journal of Sound and Vibration* 151 (1991) 9–29.
[26] P.K. Parhi, S.K. Bhattacharyya, P.K. Sinha, Hygrothermal effects on the dynamic behaviour of multiple delaminated composite plates and shells, *Journal of Sound and Vibration* 248 (2001) 195–214.
[27] J.N. Reddy, Geometrically Non-linear transient analysis of laminated composite plates, *AIAA Journal* 21 (1983) 621–629.
[28] H.U. Akay, Dynamic large deflection analysis of plates using mixed finite elements, *Computers and Structures* 11 (1980) 1–11.
[29] C.K. Chiang, C. Mei, C.E. Gray, Finite element large-amplitude free and force vibrations of rectangular thin composite plates, *Journal of Vibration and Acoustics* 113 (1991) 309–315.
[30] A. Abe, Y. Kobayashi, G. Yamada, One-to-one internal resonance of symmetric crossply laminated shallow shells, *Journal of Applied Mechanics, Transactions of the ASME* 68 (2001) 640–649.
[31] C.Y. Chia, *Non-linear Analysis of Plates*, McGraw-Hill, New York, 1980.